

A Fully Spiking Hybrid Neural Network for Energy-Efficient Object Detection

Biswadeep Chakraborty, Xueyuan She, *Student Members, IEEE*, Saibal Mukhopadhyay, *Fellow, IEEE*

Abstract—This paper proposes a Fully Spiking Hybrid Neural Network (FSHNN) for energy-efficient and robust object detection in resource-constrained platforms. The network architecture is based on Convolutional SNN using leaky-integrate-fire neuron models. The model combines unsupervised Spike Time-Dependent Plasticity (STDP) learning with back-propagation (STBP) learning methods and also uses Monte Carlo Dropout to get an estimate of the uncertainty error. FSHNN provides better accuracy compared to DNN based object detectors while being 150X energy-efficient. It also outperforms these object detectors, when subjected to noisy input data and less labeled training data with a lower uncertainty error.

Index Terms—Spiking Neural Networks, Leaky Integrate and Fire, Uncertainty Estimation, Generalization, Object Detection.

I. INTRODUCTION

Spiking Neural Networks are widely acclaimed as the third generation of neural networks given their low power consumption and close similarity in emulating how the brain works. There are two main aspects of spiking neural networks that make them attractive. Firstly, in SNNs, neurons communicate with each other through isolated, discrete electrical signals called spikes, as opposed to continuous signals, and work in continuous-time instead of discrete-time [1]. This spike-based inference methodology makes the spiking neural network energy-efficient[2]–[5]. In addition to this, spiking neural networks provides a novel unsupervised learning methodology using Spike Time Dependent Plasticity (STDP)[6]. STDP is a bio-plausible unsupervised learning mechanism that instantaneously manipulates the synaptic weights based on the temporal correlations between pre-and post-synaptic spike timings. STDP can also help improve robustness to noise in the inputs and assists in learning with less labeled data [7], [8]. These properties are attractive for real-world computer vision applications where the input can be imperfect and the labeled training data can be sparse.

The recent advances in DNN-to-SNN conversion mechanisms have enabled design of SNN with performance comparable to DNN in large datasets like ImageNet [9]. However, despite the recent developments, most of the existing works on spiking networks are primarily limited to classification. Many real-time autonomous applications such as lightweight drones and edge robots, where energy-efficient inference is crucial, have object detection as the primary task. Hence, an

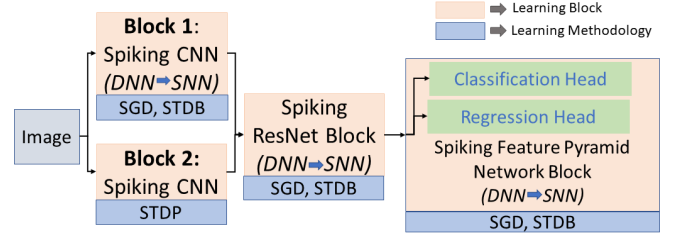


Fig. 1: General Block Diagram for Different Architectures

SNN for object detection will facilitate deployment of SNNs in such applications. Recent work on spiking based object detection [10] primarily uses the backpropagated SNN model and is trained on small networks (Tiny YOLO). This leads to a comparatively low accuracy compared to standard object detection networks. Moreover, the network does not use STDP learning limiting noise robustness or learning from less amount of labeled data.

In this paper, we propose a novel fully spiking neural network-based object detector using hybridization of unsupervised STDP based learning and supervised backpropagated learning. The proposed FSHNN network uses the baseline architecture of an object detection DNN, such as RetinaNet, as the backbone. The low-level feature space of the classifier is enhanced by fusing an auxiliary CNN block and a set of Spiking Convolution Layers pre-trained using STDP. Finally, we use a DNN-to-SNN conversion technique [11] while keeping the STDP-trained layer fixed to get the final object detector. The paper makes the following key contributions:

- We develop a fully spiking hybrid neural network for object detection integrating SGD and STDP based learning.
- We show that the STDP-based learning results in a more generalizable SNN model than a SGD-trained model.
- We adapt the Monte Carlo dropout methodology [12] to quantify uncertainty for FSHNN and use that to discriminate true positives from false-positive.
- We show that the hybridization of SGD-based and STDP-based learning within a SNN improves accuracy, improves generalizability, reduces uncertainty, and increases energy efficiency.

We evaluate the performance of FSHNN for object detection on MSCOCO dataset. Our experiments show that the FSHNN with six layers of STDP achieves an mAP of 0.426 compared to 0.388 achieved by the standard RetinaNet. We also show that FSHNN outperforms Retinanet when tested with noisy input images and trained with limited labeled data. Using the Monte Carlo Dropout method, we further demonstrate that FSHNN based object detector has a lower uncertainty compared to RetinaNet. Also, we illustrate that the FSHNN

This material is based on research supported by the Defense Advanced Research Projects Agency (DARPA) under contract number HR0011-17-2-0045. The views and conclusions contained herein are those of the authors and should not be interpreted as necessarily representing the official policies or endorsements, either expressed or implied, of DARPA.

B.Chakraborty, X.She and S. Mukhopadhyay are with the Department of Electrical and Computer Engineering, Georgia Institute of Technology, Atlanta, GA, 30332 USA e-mail:(biswadeep@gatech.edu; xshe@gatech.edu; saibal.mukhopadhyay@ece.gatech.edu)

based object detector is more generalizable compared to the standard DNN based RetinaNet. Moreover, as the network uses spiking operations during inference, it naturally enhances the energy-efficiency of object detection.

The rest of the paper is structured as follows: Section II discusses the Related Works associated with this paper; Section III revolves around the architectures and baselines used in the evaluation; Section IV deals with the Experiments undertaken and the results obtained thereby; Section V summarizes the observations and discusses the conclusions we arrived at from the experiments.

II. RELATED WORKS

A. Object Detection:

Object detection has become a critical problem of many computer vision tasks as it requires the estimation of both the category to which an object belongs and its spatial location. Single-stage detection models like Single-shot multi-box detector (SSD) [13] and YOLO [14] achieve fast inference with the cost of lower mAP and mAR. Retinanet [15] overcomes these problems as it improves on the Faster-RCNN framework with the help of a focal loss and using ResNet+FPN as the backbone network to extract features.

B. Spiking Object Detection:

Though object detection has been an important field of interest in computer vision, there is not much work for the use of spiking neural networks in object detection. Recently, Kim et al. implemented a spiking version of the YOLO object detection architecture [10]. They used channel-wise normalization and signed neurons with imbalanced thresholds to provide fast and accurate information transmission for deep SNNs. However, the proposed spiking YOLO object detector had a much lower performance than the standard DNN based YOLO and RetinaNet models.

C. DNN-to-SNN conversion:

Recent works have proposed weight normalization and threshold balancing methods to obtain minimal loss for accuracy during the conversion process. In this paper, we use the threshold balancing method [16] that gives near-lossless conversion performance for deep architectures like ResNet on complex Imagenet dataset.

D. STDP based Unsupervised learning in SNN

Spike Timing Dependent Plasticity (STDP) [17] is a variant of the Hebbian unsupervised learning algorithm. STDP describes the changes of a synaptic weight according to the relative timing of pre and post-synaptic spikes. In STDP, if a presynaptic spike precedes a post-synaptic one, a synaptic weight is potentiated.

There are various spiking neural networks (SNNs) to solve object recognition and image classification tasks by converting the traditional DNNs into spiking networks by replacing each DNN computing unit with a spiking neuron [18]. These networks aim to reduce the energy consumption in DNNs while achieving a similar accuracy score.

E. Back-propagation based Supervised Learning in SNN

Backpropagation-based supervised learning for spiking neural networks has played a critical role in improving their

performance. Rathi et. al used a hybrid training technique that combines ANN-SNN conversion and spike-based BP that reduces the latency and helps in better convergence [11]. The authors used the ANN-SNN conversion as an initialization step followed by spike-based backpropagation (STDB) incremental training. The authors also demonstrated the approach of taking a converted SNN and incrementally training it using backpropagation. This hybrid approach improves the energy-efficiency and accuracy compared to standard models trained with either only spike-based backpropagation or only converted weights.

F. Generalizability of Neural Networks

Recent works [19]–[21] have analyzed overparameterized (wide) neural networks from a theoretical perspective by connecting them to reproducing kernel Hilbert spaces. The papers have also shown that under proper conditions, the weights of a well-trained overparameterized network remain very close to their initialization. Thus, during training the model searches within some class of reproducing kernel functions, where the associated kernel is called the “neural tangent kernel” which only depends on the initialization of the weights.

Another line of research has worked on comparing the generalization error while using different training strategies [22]. The authors show that we can control the generalization error of a training algorithm using the Hausdorff dimension of its trajectories. Gurbuzbalaban et al. showed that depending on the structure of the Hessian of the loss at the minimum, and the choices of the algorithm parameters η, b , the SGD iterates will converge to a heavy-tailed stationary distribution [23].

Recent works have worked on determining the generalization characteristics of the object proposal generation that is the first step in detection models [24]. A more generalizable object proposal can help to scale detection models to a larger number of classes with fewer annotations. Thus, the paper studies how a detection model trained on a small set of source classes can provide proposals that generalize to unseen classes.

III. MOTIVATIONS

In this section, we discuss the primary motivations for using a hybrid spiking neural network based object detector. We discuss the generalization advantages we can obtain by fusing features learned using STDP with the SGD process.

A. Transfer Learning and Feature Fusion

In this subsection, we motivate the feature fusion of STDP and SGD processes for object detection. We argue that features learned using STDP can complement the standard SGD and making the training simpler, more generalizable, and robust. Zeiler et. al. observed that the lower layers of a DNN converged much faster compared to the higher layers [25]. Also, they showed that small transformations in the input image impact the lower layers more than higher layers. Recent works have empirically demonstrated that a convolutional network trained on a large dataset can be successfully generalized to other tasks where less data is available [26]. These observations motivated us to use additional layers in the initial stages of the backbone classifier to capture the low-level features. Donahue et al. showed that lower level features can be transferred to different networks to get superior performance [27]. Developing on these ideas, we utilize the

spiking convolutional layers trained using the unsupervised STDP method since it can better apprehend local features compared to the standard DNN.

In addition to this, Jacot et al. showed that the generalizability of an infinitely wide neural network is dependent on the initialization and a better initialization improves the generalizability of the network [19]. Thus, we show the generalizability of STDP compared to SGD that would subsequently motivate us to demonstrate the generalization of spiking models.

B. Generalizability of STDP

In this subsection, we compare the generalization bounds of a spiking convolutional neural network to its DNN counterpart with the same architecture. Jacot et al. showed that the generalizability of an infinitely wide neural network is dependent on the initialization and a better initialization improves the generalizability of the network [19]. Hence, we study the generalizability of STDP compared to SGD that would subsequently motivate us to demonstrate the generalization of spiking models.

Simsekli et al. demonstrated that the generalization error is controlled by the uniform Hausdorff dimension of the learning algorithm, with the constants inherited from the regularity conditions [22]. Authors further showed that the Hausdorff dimension is controlled by the tail behavior of the process, with heavier-tails implying less generalization error. Therefore, we study the Hausdorff dimensions of the trajectories of the STDP and SGD learning methodologies.

Recent literatures have shown that the STDP based learning in SNN follow an Ornstein–Uhlenbeck process [28]. On the other hand, SGD follows a Feller process [29]. So, we compare the tail indices of the two stochastic processes to study their heavy-tailed natures.

We use stochastic differential equations (SDEs) to formulate local plasticity rules for parameters θ_i that control synaptic connections (if $\theta_i > 0$) and synaptic weights $w_i = \exp(\theta_i - \theta_0)$

$$d\theta_i = \left(b \frac{\partial}{\partial \theta_i} \log p^*(\theta) \right) dt + \sqrt{2Tb} \cdot d\mathcal{W}_i$$

where $d\mathcal{W}_i$ denotes an infinitesimal (1)

step of a random walk (Wiener process), drift diffusion b = learning rate, T = temperature ($T=1$ until last slide)

The Fokker-Planck (FP) equation tracks the resulting evolution of the SNN configurations θ over time, yielding the stationary distribution $\frac{1}{Z} p^*(\theta)^{1/T}$ which follows the Ornstein–Uhlenbeck process [28]

$$\begin{aligned} \frac{\partial}{\partial t} p_{FP}(\theta, t) = \sum_i - \frac{\partial}{\partial \theta_i} \left(\left(b \frac{\partial}{\partial \theta_i} \log p^*(\theta) \right) p_{FP}(\theta, t) \right) \\ + \frac{\partial^2}{\partial \theta_i^2} (Tb p_{FP}(\theta, t)) \end{aligned} \quad (2)$$

The practically relevant forms of the target distribution $p^*(\theta)$ of network configurations depend on the type of learning. For this case, we consider the unsupervised learning method described in [30]. We perform a tail index analysis of STDP in deep SNN, similar to the method adopted in [31].

Several methods works have explored estimation of the tail-index of an extreme-value distribution [32], [33]. However, most of these methods fail to estimate the tail index of α -stable distributions [34], [35]. We consider the estimation method proposed by Mohammadi et. al. [36] which has a faster convergence rate and smaller asymptotic variance than the aforementioned methods. The basic approach is discussed below. It gives a class of estimators based on quantiles

In the following, $f_X(\cdot)$ and $F_X(\cdot)$ denote the probability density function and distribution function of a random variable X , respectively, and ξ_p^X satisfies $p = P(X \leq \xi_p^X)$.

We know for the one-dimensional case, if X_1, \dots, X_n be a sequence of i.i.d. random variables with probability density function $f_X(\cdot)$, and $X_{1:n} \leq \dots \leq X_{n:n}$, $\frac{j}{n} \rightarrow p \in (0, 1)$, then

$$\lim_{n \rightarrow +\infty} \sqrt{n} (X_{j:n} - \xi_p^X) \rightarrow_D N \left(0, \frac{p(1-p)}{(f_X(\xi_p^X))^2} \right) \quad (3)$$

where " \rightarrow_D " denotes convergence in distribution.

We consider $|X|_{1:n} \leq \dots \leq |X|_{n:n}$ such that $|x| = \left(\sum_{k=1}^d x_k^2 \right)^{1/2} \forall x = (x_1, \dots, x_d) \in \mathbb{R}^d$. Consider an i.i.d. sequence of strictly α -stable random vectors $\mathbf{X}_i, i = 1, 2, \dots, m$ with dimension $d \geq 1$. Let $\mathbf{Y} = \sum_{i=1}^m \mathbf{X}_i$. As Mohammadi et. al. has shown [36],

$$\left(\xi_p^{\log|\mathbf{Y}|} - \xi_p^{\log|\mathbf{X}_1|} \right) / \log m = 1/\alpha$$

These relations were used to construct an estimator for $1/\alpha$ as follows:

Let $\{\mathbf{X}_i\}_{i=1}^K$ be a collection of random variables with $\mathbf{X}_i \sim \mathcal{S}_\alpha \mathcal{S}(\sigma)$ and $K = K_1 \times K_2$. Define $Y_i \triangleq \sum_{j=1}^{K_1} X_{j+(i-1)K_1}$ for $i \in [1, K_2]$. Then, the estimator

$$\hat{\frac{1}{\alpha}} \triangleq \frac{1}{\log K_1} \left(\frac{1}{K_2} \sum_{i=1}^{K_2} \log |Y_i| - \frac{1}{K} \sum_{i=1}^K \log |X_i| \right) \quad (4)$$

converges to $1/\alpha$ almost surely, as $K_2 \rightarrow \infty$.

In order to estimate the tail-index α at iteration k , we first partition the set of data points $\mathcal{D} \triangleq \{1, \dots, n\}$ into many disjoint sets $\Omega_k^i \subset \mathcal{D}$ of size b , such that the union of these subsets give all the data points. Formally, for all $i, j = 1, \dots, n/b$, $|\Omega_k^i| = b$, $\cup_i \Omega_k^i = \mathcal{D}$, and $\Omega_k^i \cap \Omega_k^j = \emptyset$ for $i \neq j$. We then compute the full gradient $\nabla f(\mathbf{w}_k)$ and the stochastic gradients $\nabla \tilde{f}_{\Omega_k^i}(\mathbf{w}_k)$ for each minibatch Ω_k^i . Finally, we compute the stochastic gradient noises $U_k^i(\mathbf{w}_k) = \nabla \tilde{f}_{\Omega_k^i}(\mathbf{w}_k) - \nabla f(\mathbf{w}_k)$, vectorize each $U_k^i(\mathbf{w}_k)$ and concatenate them to obtain a single vector, and compute the reciprocal of the estimator given in Eq. 4. We use $K = pn/b$ and K_1 is the divisor of K that is the closest to \sqrt{K} for our experiments.

Similar to the analysis done by Simsekli et. al, we evaluate the tail-index of the standard CNN trained with the SGD and the spiking convolutional neural networks trained with STDP processes [31]. The experiment is repeated with varying numbers of layers and is evaluated on the MNIST dataset and the tail indices are reported in Table I. We observe that the STDP process has a smaller value of α for each of the cases thus implying that the distribution has a heavier tail and thus is more generalizable.

TABLE I: Comparison of Tail Indices α of SGD, STDP for varying depth in Convolutional Networks[31]

No. of Layers	SGD	STDP
3	1.297	1.206
4	1.291	1.193
5	1.284	1.188
6	1.273	1.181

IV. ARCHITECTURES

In this section, we introduce the novel Fully Spiking Hybrid Neural Network-based Object Detector. Since fusion improves learning ability of low-level features and STDP is more generalizable than SGD, we introduce a model that fuses the STDP and the SGD based learning methods.

A. Fully Spiking Hybrid Object Detector Architecture

For the FSHNN based Object Detector model, we take the DNN based Retinanet model[15] with a backbone network of ResNet 101. We augment the ResNet layers with an Auxilliary CNN block and an STDP block as shown in Fig. 1. We keep the STDP block frozen and convert the rest of the DNN to a Spiking network using a DNN to SNN conversion method as described in [11]. Hence, we get a fully spiking object detector with augmented STDP layers and an auxiliary CNN block in the backbone. The motivation for such a model is to compare the benefits of adding an unsupervised training methodology in the object detection network.

For this paper, we use a ResNet 101 as the backbone network. For Block1 in FSHNN, we use a block of four spiking convolutional neural networks converted from their DNN counterparts. Block 2 for FSHNN is composed of the STDP layers. As we repeat the experiments with multiple STDP layers, we keep on increasing a 64×64 filter in each case at the end of the last Spiking Convolutional Layer in Block 2 as shown in Fig 1. The detailed filter sizes for the Blocks 1,2 and the ResNet are given in Fig 2 and [15] respectively.

B. STDP based Spiking CNN architecture

The architecture of the unsupervised STDP based convolutional module is shown in Fig. 3. The architecture differs from the conventional DNN based architectures in following respects. First, we use the 8-bit pixel intensity values of the input image to generate the spike train that is then given to the spiking neurons of the Spiking Convolutional Layer as inputs. The connections are made with plastic synapses following the STDP learning rule. When the neuron in the SCNN layer spikes, an inhibitory signal is sent to the neurons at the same spatial coordinates across all depths in the same layer. This inhibition facilitates the neurons at the same location to learn different features and thus, achieves a competitive local learning behavior of robust low-level features. Another problem in multi-layered SNNs is that a spiking neuron needs several spikes to emit a single spike that leads to diminishing spiking frequency. To tackle this problem, we use a layer-wise learning procedure where after learning in the first layer is complete, its cross-depth inhibition is disabled while keeping its conductance matrix fixed. Hence, the spiking threshold for the neurons in the first layer is lowered to provide a higher spiking frequency. In this way, the neurons in the first layer

receive input from the images and produce spikes that in turn facilitate the learning in the second layer and so on.

C. Learning Methodology

We train the FSHNN model in a two-step procedure. Firstly, we train the STDP block independently as a separate neural network as shown in Fig 3 on the ImageNet traffic dataset. Hence, we use these pre-trained STDP layers as a supplement to the ResNet backbone as described above. Hence, with these STDP layers frozen in place, we use the DNN to SNN conversion process and using the weights obtained as an initialization point, we retrain these other supervised spiking layers using the STDB process[11]. This process enables us to achieve higher accuracy in a shorter time-step. As such, we get a fully spiking Retinanet with the pre-trained STDP layers in the backbone. This network is then again retrained using the STBP method to achieve the final trained model.

D. Model Uncertainty in Spiking Object Detectors

1) Monte Carlo Dropout for Spiking Neural Networks

Recent work has shown that the use of dropout during training can be used as an approximation of the Monte Carlo simulation, thus giving us an estimate of the Bayesian inference done on the network [37]. Lee et al [38] introduced the dropout technique for spiking networks, though they used it only during training and not for inference. In this paper, we use the dropout during both training and inference so that inference with dropout enabled can be interpreted as an approximate Bayesian Inference in deep Gaussian processes, similar to its DNN counterpart.

The dropout method in SNNs differs from that in the standard DNNs where each epoch of training has several iterations of mini-batches and during each iteration, randomly selected units are disconnected from the network while weighting by its posterior probability. On the other hand, in SNNs, each iteration has more than one forward propagation depending on the time length of the spike train. Thus, the output error is back-propagated and the network parameters are modified only at the last time step. Also, during training, the set of connected units within an iteration of mini-batch data remains the same in such a way that the same random subset of units constitutes the neural network during each forward propagation within a single iteration. Similarly, during inference also, we take a random subset of the entire network in a single iteration and each iteration has multiple forward passes. Thus, we use multiple such forward samples and partition the individual detections into observations as discussed in [39] to obtain the label uncertainty and the spatial bounding box uncertainty estimates.

2) Epistemic Uncertainty Estimation for Object Detectors

Object Detection is concerned with estimating a bounding box alongside a label distribution for multiple objects in a scene. We extend the concept of Dropout Sampling as a means to perform tractable variational inference from image recognition to object detection. We employ the dropout sampling approximation method as described in [37] to sample from the distribution of weights $p(\mathbf{W} \mid \mathbf{T})$ where \mathbf{W} are the learned weights of the FSHNN detection network and \mathbf{T} is the training data. We apply MC Dropout treating the object detector as

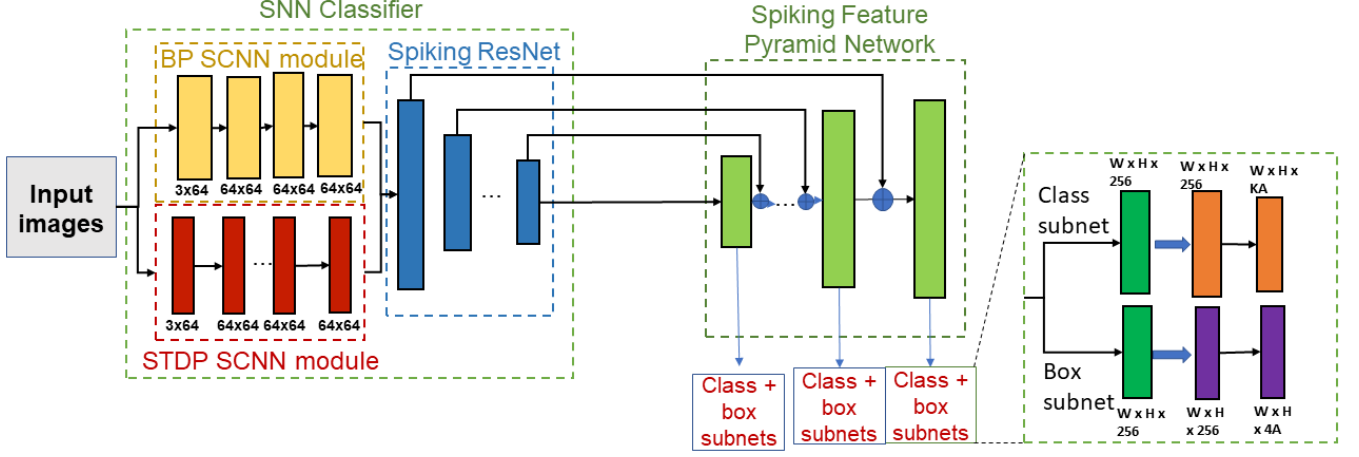


Fig. 2: Architectural block diagram showing the different parts of the FSHNN spike based object detector with varying STDP layers

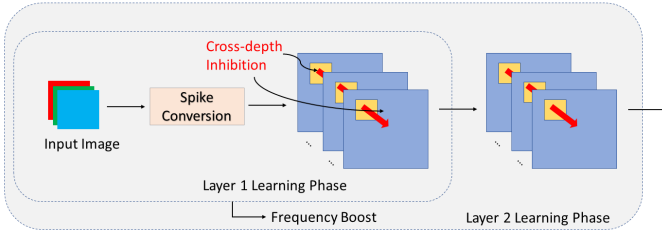


Fig. 3: The architecture of the spiking convolutional module for feature extraction and layer-by-layer learning process

a black box [39]. Uncertainty is then estimated as sample statistics from spatially correlated detector outputs.

In the object detectors, we use the dropout layers after each of the convolution layer in the main ResNet block in the backbone network. This modified network is trained with the dropout layers as discussed above. With these trained layers, we use the dropout during inference which acts as a Monte Carlo Sampling technique. Every forward pass through the network corresponds to performing inference with a different network $\tilde{\mathbf{W}}$ which is approximately sampled from $p(\mathbf{W}|\mathbf{T})$.

V. EXPERIMENTAL RESULTS

In this section, we present experimental results to evaluate performance of FSHNN. First, we evaluate the performance of FSHNN on the MS-COCO dataset [40]. The MS COCO dataset that has 223K frames with instances from 81 different object categories, and a training/testing split of 118K/5K. Second, we evaluate performance of FSHNN considering varying input noise levels and training the models on limited labeled data. Third, we compare FSHNN to other spiking and non-spiking object detectors trained using backpropagation considering object detection performance and energy efficiency. Finally, we also showed that the object proposal of the FSHNN based object detector generalizes better for unseen data classes in comparison to the standard object detectors like RetinaNet.

A. Evaluation Metrics

The two main evaluation metrics are used to quantify the performance of object detectors discussed above are:

- 1) *Mean Average Precision (mAP)* : is an accepted metric for evaluating object detection performance. mAP measures a detector's ability to detect all objects in a closed set dataset with a correct classification and accurate localization ($\text{IoU} \geq 0.5$), while minimizing incorrect detections and their confidence score. For performance on the detection task, we use the Mean Average Precision (mAP) at 0.5 IOU. The maximum mean average precision achievable by a detector is 100%.
- 2) *Uncertainty Error (UE)* [41]: This metric represents the ability of an uncertainty measure to accept correct detection and reject incorrect detection. The uncertainty error is the probability that a detection is incorrectly accepted or rejected at a given uncertainty threshold. We use the Minimum Uncertainty Error (MUE) at 0.5 IOU to determine the ability of the detector's estimated uncertainty to discriminate true positives from false positives. The lowest MUE achievable by a detector is 0%. We define the Categorical MUE (CMUE) since we are using the Categorical entropy and finally, we average the CMUE overall categories in a testing dataset to derive the Mean (Categorical) MUE (mCMUE).

B. Performance Evaluation of FSHNN

In this section, we evaluate the performance of the FSHNN based object detector on the MS-COCO dataset. We do so by performing three separate experiments. First, we evaluate the performance of the model under normal circumstances, train with all the input data, and test with clean images. We repeat this experiment for multiple STDP layers in the **Block 2**, as shown in Fig. 1. The results are summarized in Table II. Fig. 5 demonstrates the performance of the FSHNN object detector for clean and noisy input image.

We see that the insertion of more STDP layers reduces both classification and regression losses, but the classification loss reduce more. Also, from Fig. 4, we see that the inclusion of

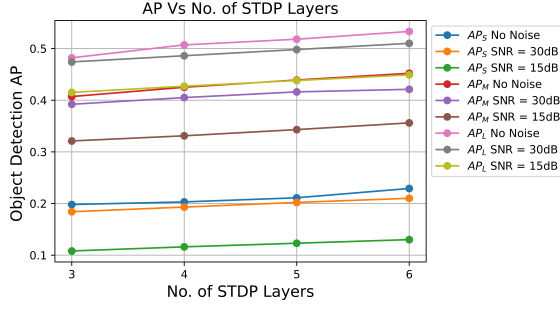


Fig. 4: Figure showing the change of small, medium and large object detection AP with increasing number of STDP layers

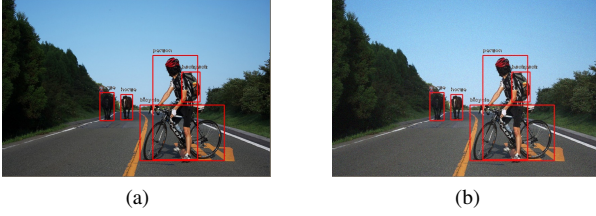


Fig. 5: FSHNN object detector performance on (a) clean and (b) noisy image

the STDP layers increases the AP for all small, medium and large object detections.

1) Performance with Input Noise in Testing

We evaluate the average precision and recall of the proposed FSHNN based object detector on the MS-COCO dataset under the signal-to-noise ratios (S.N.R) of 30dB and 15dB. The results of the experiments are summarized in Table III. We see an increment of 12% on the addition of 3 new STDP layers for the no noise case. The addition of STDP layers play a more significant role as the network is subjected to more adversarial conditions like for example, when there is an increase in the input noise level or the network is trained with lesser amount of labelled training data.

2) Performance after Training with Less Data

To further demonstrate the robustness of the FSHNN object detector, we evaluated it with restrained training. We train the model on a partial MS COCO dataset and reported the average precision and recall. We see that the object detectors with more STDP layers perform better especially when significant amounts of data are removed during training. Thus, we may conclude that the STDP layers trained with unlabelled data learn critical features for classification as can be seen from the decrease in classification loss with increasing STDP layers in Table III.

C. Comparison with Baselines

We compare performance and energy-efficiency of FSHNN with different baselines. The two baseline models for this comparison are described as follows (Table IV):

- 1) *RetinaNet*. RetinaNet is a state-of-the-art DNN based object detector that works using the Focal Pyramid Network architecture. In this paper, we are using ResNet 101 as the backbone network for the RetinaNet object detector.

- 2) *Back Propagated Fully Spiking Object Detector*. For the backpropagated fully spiking RetinaNet we replace the STDP layers (Block 1 in Fig 1) in the FSHNN based object detector with corresponding DNN layers. For this experiment, we have replaced 3 STDP layers with 3 Convolution Layers. Hence, we use a similar DNN-to-SNN conversion methodology to obtain a Fully Spiking Object Detector with backpropagated spiking layers with the same architecture as FSHNN based object detector. With the weights obtained in this conversion process as the initialization point, we retrain the model using STBP to get the final trained model.

1) Performance Comparison

We perform a two-fold evaluation of the FSHNN model with the baselines described above - first we evaluate the performance of the object detectors without any perturbation and train with the full training dataset. The results are represented in Tab. V. We see that though the FSHNN with 3 STDP layers performs closely to the RetinaNet, the FSHNN with 6 STDP layers outperforms the RetinaNet with respect to both mAP/mAR and uncertainty error.

We test the robustness of the model by testing the model with different adversarial conditions - first, we use two different noise levels (SNR = 30dB, 15dB) and also evaluate the performance after training the model with increasingly limited labeled data (80%, 60%, and 40% data respectively).

We observe that in the no noise scenario, the FSHNN with 6 STDP layers outperforms the RetinaNet, and the difference in their performances increases as the input noise level is increased. Further, when the models are trained with a lesser amount of labeled data, even the FSHNN with 3 STDP layers perform better than the baseline ones.

2) Energy Efficiency

We next compare the energy advantage of spiking models (FSHNN and Backpropagated spiking layer) with Retinanet (Table VIII). As expected from prior works, [3], [4] we observe that the spiking neural network-based object detector consumes significantly less power than the standard models while providing comparable (backpropagated spiking) or better performance. First, most operations in DNNs occur in convolutional layers where the multiply-accumulate (MAC) operations are primarily responsible during execution. However, SNNs perform accumulate (AC) operations because spike events are binary operations whose input is integrated into a membrane potential only when spikes are received. For a fair comparison, we focused solely on computational power (MAC and AC) used for object detection on a single image.

Horowitz et. al. [42] showed that a 32-bit floating-point (FL) MAC operation consumes 4.6 pJ (0.9 + 3.7 pJ) and 0.9 pJ for an AC operation. A 32-bit integer (INT) MAC operation consumes 3.2 pJ (0.1 + 3.1 pJ) and 0.1 pJ for an AC operation. Based on these measures, we calculated the energy consumption of the spiking object detectors by multiplying FLOPS (floating-point operations) and the energy consumption of MAC and AC operations calculated. The FLOPS for the different architectures described in the paper is given in Table VIII shows that FSHNN and the other spiking object detectors demonstrate better energy efficiency for 32-

TABLE II: Table showing Performance of the FSHNN based Object Detector with Increasing STDP Layers

Number of STDP Layers	Classification Loss	Regression Loss	mAP	AP _S	AP _M	AP _L	mAR	AR _S	AR _M	AR _L	mCMUE
3	0.4127	0.6912	0.379	0.198	0.407	0.482	0.492	0.292	0.554	0.615	0.251
4	0.3841	0.6787	0.392	0.203	0.425	0.507	0.515	0.308	0.578	0.635	0.244
5	0.3352	0.6536	0.409	0.211	0.439	0.518	0.527	0.316	0.591	0.652	0.236
6	0.3076	0.6193	0.426	0.229	0.452	0.533	0.541	0.327	0.612	0.668	0.229

TABLE III: Table showing Robustness of FSHNN based Object Detector for Noisy Testing Data and Limited Labelled Training Dataset

# of STDP Layers	Classification Loss	Regression Loss	mAP	mAR	cMUE
SNR = 30dB					
3	0.4318	0.7165	0.368	0.483	0.317
4	0.3987	0.7093	0.382	0.497	0.305
5	0.3516	0.6845	0.395	0.519	0.291
6	0.3204	0.6522	0.412	0.531	0.284
SNR = 15dB					
3	0.6723	0.7345	0.305	0.441	0.455
4	0.6552	0.7269	0.316	0.453	0.448
5	0.6218	0.7114	0.324	0.465	0.439
6	0.6014	0.7008	0.331	0.476	0.431
80% Training Data					
3	0.4157	0.6998	0.358	0.473	0.301
4	0.3806	0.6742	0.363	0.481	0.289
5	0.3694	0.6516	0.392	0.514	0.214
6	0.3356	0.6288	0.411	0.547	0.199
60% Training Data					
3	0.4975	0.7884	0.329	0.431	0.390
4	0.4698	0.7545	0.348	0.476	0.358
5	0.4513	0.7312	0.364	0.493	0.317
6	0.4027	0.7084	0.396	0.518	0.296
40% Training Data					
3	0.6057	0.9432	0.287	0.386	0.513
4	0.5964	0.9303	0.296	0.401	0.501
5	0.5837	0.9268	0.308	0.415	0.486
6	0.5759	0.9115	0.322	0.426	0.478

TABLE IV: Table Describing the Learning Blocks used in the Architectures

		Block 1	Block 2	ResNet Block	FPN Block
Retinanet	Layer	None	None	CNN	CNN
	Learning	N/A	N/A	BP	BP
FSHNN Obj Det	Layer	SNN	SNN	SNN	SNN
	Learning	BP	STDP	BP	BP
BP Spiking Obj Det	Layer	SNN	SNN	SNN	SNN
	Learning	BP	BP	BP	BP

bit FL and INT operations. Total inference energy E for ANN/SNN considering FLOPS count across all N layers of a network is defined as [2]

$$E_{ANN} = \left(\sum_{i=1}^N FLOPS_{ANN} \right) * E_{MAC} \quad (5)$$

$$E_{SNN} = \left(\sum_{i=1}^N FLOPS_{SNN} \right) * E_{AC} * T$$

For SNN, the energy calculation considers the latency incurred as the rate-coded input spike train has to be presented over T time-steps to yield the final prediction result. Since we are also using a similar training methodology using STDB, we have too considered the number of time steps $T = 300$ in this paper [11].

3) Generalizability of Object Proposal

As defined by Wang et. al, the generalizability of an object detector model is its ability to localize (not classify) unanno-

tated objects in the training dataset [24]. For this experiment, we randomly split the MS-COCO dataset into two parts - the source dataset consisting of 70 seen classes and the target dataset of 10 unseen classes. We use the target dataset to evaluate the generalization of the proposal model trained with the source dataset. The train split is utilized for training and the 5000 images from the validation set during evaluation.

To evaluate the quality of the proposals, we use the standard average recall (AR@k) [43]. One of the primary motivations for building a generalized proposal model is to use the resulting proposals to train detection models for unseen classes with limited or no bounding box annotation.

We compare the generalization ability of the FSHNN based object detector and RetinaNet in Fig. 6. The models are trained on the COCO-source-train dataset as described above. We report AR@100 on seen classes in the COCO-source-test dataset and unseen classes in the COCO-target-test. We build on the hypothesis that the difference in performance between seen and unseen classes reflects the generalization gap. We also show an upper-bound performance on COCO-target-test obtained by models trained on the full training dataset containing both COCO-source-train and COCO-target-train. On seen classes, RetinaNet achieves a worse performance compared to FSHNN (a drop of 7.01%). However, the drop is larger for unseen target classes (a drop of 11.9%), indicating a larger generalization gap for RetinaNet. One reason for this is that RetinaNet is more sensitive to missing bounding boxes corresponding to unlabelled unseen classes in the source dataset. Also, since RetinaNet uses focal-loss, the unseen and unannotated object classes proposals in the training data are treated as hard-negatives. Thus, the model heavily penalizes proposals corresponding to unannotated bounding boxes, leading to an overall decrease in AR. Since some seen classes share visual similarity with unseen classes, this sensitivity to missing annotations also affects AR for seen classes. However, this effect is more magnified for unseen target classes. On the other hand, in FSHNN, only a small number of proposals that do not intersect with annotated bounding boxes are sampled at random as negatives. Hence, the probability that a proposal corresponding to an unseen object class is negative is lower, leading to better generalization. Thus, we observe that the detection head of FSHNN provides better overall performance without sacrificing generalization.

D. Comparison to Spiking Yolo

We compare FSHNN model performance with the state-of-art spike-based object detector - Spiking YOLO [10]. Though both of them are fully spiking object detectors, there are a few key differences between the two. First, the Spiking Yolo is composed of backpropagated Spiking Convolution Layers that are trained using supervised learning. In contrast, FSHNN

TABLE V: Table showing the performance of the different object detectors

	mAP	AP _S	AP _M	AP _L	mAR	AR _S	AR _M	AR _L	mCMUE
No Noise; 100% Training Data									
RetinaNet	0.388	0.207	0.420	0.498	0.501	0.301	0.566	0.624	0.237
BP Spiking Obj Detector	0.375	0.189	0.401	0.477	0.486	0.283	0.549	0.598	0.254
FSHNN Obj Det (3 STDP layers)	0.379	0.198	0.407	0.482	0.492	0.292	0.554	0.615	0.251
FSHNN Obj Det (6 STDP layers)	0.426	0.223	0.452	0.526	0.541	0.312	0.611	0.682	0.229

TABLE VI: Table showing the performance of the different object detectors with input noise during testing

	mAP	AP _S	AP _M	AP _L	mAR	AR _S	AR _M	AR _L	mCMUE
SNR = 30dB									
RetinaNet	0.371	0.183	0.409	0.481	0.489	0.279	0.554	0.613	0.313
BP Spiking Obj Detector	0.365	0.186	0.388	0.472	0.478	0.278	0.543	0.589	0.320
FSHNN Obj Det (3 STDP layers)	0.368	0.190	0.395	0.476	0.483	0.285	0.549	0.605	0.317
FSHNN Obj Det (6 STDP layers)	0.412	0.211	0.446	0.482	0.531	0.308	0.599	0.668	0.284
SNR = 15dB									
RetinaNet	0.277	0.104	0.237	0.349	0.416	0.204	0.401	0.426	0.605
BP Spiking Obj Detector	0.297	0.159	0.347	0.406	0.428	0.248	0.473	0.539	0.483
FSHNN Obj Det (3 STDP layers)	0.305	0.163	0.358	0.417	0.441	0.257	0.496	0.553	0.455
FSHNN Obj Det (6 STDP layers)	0.331	0.184	0.392	0.451	0.476	0.271	0.528	0.587	0.431

TABLE VII: Table showing the performance of the different object detectors with input noise during testing

	mAP	AP _S	AP _M	AP _L	mAR	AR _S	AR _M	AR _L	mCMUE
80% training set									
RetinaNet	0.376	0.189	0.398	0.478	0.481	0.287	0.543	0.608	0.308
BP Spiking Obj Detector	0.353	0.178	0.379	0.460	0.468	0.264	0.525	0.574	0.305
FSHNN Obj Det (3 STDP layers)	0.358	0.182	0.386	0.466	0.473	0.274	0.538	0.591	0.301
FSHNN Obj Det (6 STDP layers)	0.411	0.221	0.452	0.521	0.547	0.311	0.594	0.662	0.199
60% training set									
RetinaNet	0.328	0.137	0.342	0.431	0.433	0.231	0.492	0.557	0.393
BP Spiking Obj Detector	0.316	0.129	0.328	0.424	0.423	0.221	0.476	0.541	0.396
FSHNN Obj Det (3 STDP layers)	0.329	0.140	0.341	0.435	0.431	0.235	0.488	0.552	0.390
FSHNN Obj Det (6 STDP layers)	0.396	0.188	0.409	0.496	0.518	0.271	0.542	0.608	0.296
40% training set									
RetinaNet	0.234	0.056	0.266	0.351	0.349	0.158	0.413	0.472	0.799
BP Spiking Obj Detector	0.254	0.076	0.262	0.368	0.365	0.163	0.412	0.487	0.613
FSHNN Obj Det (3 STDP layers)	0.287	0.103	0.297	0.399	0.396	0.192	0.449	0.518	0.513
FSHNN Obj Det (6 STDP layers)	0.322	0.126	0.337	0.439	0.426	0.221	0.492	0.553	0.478

couples both STDP based unsupervised learning methodologies with backpropagation learning. This helps the FSHNN network achieve high performance as well as robustness against input noise and less labeled data for training. Second, we analyze the uncertainty and generalizability properties of FSHNN; but such analyses were not performed for spiking YOLO[10]. Third, FSHNN shows a higher performance than spiking YOLO. While the spiking YOLO reported an mAP of 26.24% [10], the FSHNN network with 6 STDP layers described in this paper achieves an mAP of 42.6%. We note that the spiking YOLO object detector is based on the YOLO architecture. The YOLO architecture suffers from an extreme class imbalance where the detectors evaluate a lot of extra

candidate locations a majority of which do not contain an object. In contrast, FSHNN uses the RetinaNet architecture that fixes this issue by using the Focal Pyramid Network and the Focal Loss. The Spiking YOLO is based out of the Tiny YOLO object detector architecture which uses 6.97×10^9 FLOPS of computation while the channel-norm based spiking YOLO as described in the paper uses 4.9×10^7 FLOPS of computation in 3500 time steps. Thus the theoretical energy efficiency achieved using the Spiking YOLO is only $1.3x$. It must be noted here that the proposed FSHNN based object detectors use almost 4x number of FLOPS. However, the use of the STDB method greatly reduces the time steps needed from 3500 to just 300 as used in this paper. This leads to the

TABLE VIII: Table showing the energy efficiency of spiking neural object detectors

	Param(M)	FLOPS	$EE = \frac{EE_{ANN}}{EE_{SNN}}$
RetinaNet	52.78	262.81×10^9	N/A
BP Spiking Obj Det	52.99	1.85×10^8	151.53
FSHNN Obj Det (3 layers STDP)	52.96	1.81×10^8	154.88
Ablation Studies			
FSHNN Obj Det (4 layers STDP)	53.04	1.84×10^8	152.35
FSHNN Obj Det (5 layers STDP)	53.08	1.88×10^8	149.11
FSHNN Obj Det (6 layers STDP)	53.11	1.90×10^8	147.54

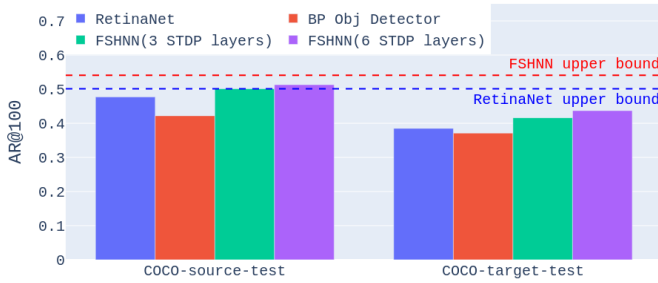


Fig. 6: AR@100 corresponding to different models trained on COCO-source-train and evaluated on different test splits. Upper-bound corresponds to model trained on full COCO dataset and evaluated on COCO-target-test.

huge difference in energy efficiency in the two models.

VI. CONCLUSION

We have presented fully spiking hybrid neural network (FSHNN), a novel spiking neural network based object detector by fusing features extracted from both unsupervised STDP based learning and supervised backpropagation based learning. We have also developed used a MC dropout based sampling method to estimate the uncertainty of FSHNN. Experimental results on MSCOCO dataset shows that the FSHNN demonstrates comparable or better performance than standard DNN while promising orders of magnitude improvement in energy-efficiency. Further, we have observed that FSHNN network outperforms the baseline DNN as well as a spiking network trained with backpropagation when tested under input noise or trained with less available labelled data. We have also shown that integration of STDP learning helps improve generalization ability of FSHNN. In conclusion, we demonstrated the feasibility of designing a fully spiking network for object detection facilitating the deployment spiking networks for resource-constrained environments.

REFERENCES

- [1] W. Maass, "Networks of spiking neurons: the third generation of neural network models," *Neural networks*, vol. 10, no. 9, pp. 1659–1671, 1997.
- [2] P. Panda, S. A. Aketi, and K. Roy, "Toward scalable, efficient, and accurate deep spiking neural networks with backwired residual connections, stochastic softmax, and hybridization," *Frontiers in Neuroscience*, vol. 14, 2020.
- [3] J. V. Stone, "Principles of neural information theory," *Computational Neuroscience and Metabolic Efficiency*, 2018.

- [4] P. A. Merolla, J. V. Arthur, R. Alvarez-Icaza, A. S. Cassidy, J. Sawada, F. Akopyan, B. L. Jackson, N. Imam, C. Guo, Y. Nakamura *et al.*, "A million spiking-neuron integrated circuit with a scalable communication network and interface," *Science*, vol. 345, no. 6197, pp. 668–673, 2014.
- [5] S. Carrillo, J. Harkin, L. McDaid, S. Pande, S. Cawley, B. McGinley, and F. Morgan, "Advancing interconnect density for spiking neural network hardware implementations using traffic-aware adaptive network-on-chip routers," *Neural networks*, vol. 33, pp. 42–57, 2012.
- [6] T. V. Bliss and G. L. Collingridge, "A synaptic model of memory: long-term potentiation in the hippocampus," *Nature*, vol. 361, no. 6407, pp. 31–39, 1993.
- [7] A. Tavanaei and A. S. Maida, "Bio-inspired spiking convolutional neural network using layer-wise sparse coding and stdp learning," *arXiv preprint arXiv:1611.03000*, 2016.
- [8] P. Panda and N. Srinivasa, "Learning to recognize actions from limited training examples using a recurrent spiking neural model," *Frontiers in neuroscience*, vol. 12, p. 126, 2018.
- [9] J. Deng, W. Dong, R. Socher, L.-J. Li, K. Li, and L. Fei-Fei, "Imagenet: A large-scale hierarchical image database," in *2009 IEEE conference on computer vision and pattern recognition*. Ieee, 2009, pp. 248–255.
- [10] S. Kim, S. Park, B. Na, and S. Yoon, "Spiking-yolo: Spiking neural network for energy-efficient object detection," in *Proceedings of the AAAI Conference on Artificial Intelligence*, vol. 34, no. 07, 2020, pp. 11 270–11 277.
- [11] N. Rathi, G. Srinivasan, P. Panda, and K. Roy, "Enabling deep spiking neural networks with hybrid conversion and spike timing dependent backpropagation," *arXiv preprint arXiv:2005.01807*, 2020.
- [12] B. Nessler, M. Pfeiffer, L. Buesing, and W. Maass, "Bayesian computation emerges in generic cortical microcircuits through spike-timing-dependent plasticity," *PLoS Comput Biol*, vol. 9, no. 4, p. e1003037, 2013.
- [13] W. Liu, D. Anguelov, D. Erhan, C. Szegedy, S. Reed, C.-Y. Fu, and A. C. Berg, "Ssd: Single shot multibox detector," in *European conference on computer vision*. Springer, 2016, pp. 21–37.
- [14] J. Redmon and A. Farhadi, "Yolov3: An incremental improvement," *arXiv preprint arXiv:1804.02767*, 2018.
- [15] T.-Y. Lin, P. Goyal, R. Girshick, K. He, and P. Dollár, "Focal loss for dense object detection," in *Proceedings of the IEEE international conference on computer vision*, 2017, pp. 2980–2988.
- [16] A. Sengupta, Y. Ye, R. Wang, C. Liu, and K. Roy, "Going deeper in spiking neural networks: Vgg and residual architectures," *Frontiers in neuroscience*, vol. 13, p. 95, 2019.
- [17] S. Huang, C. Rozas, M. Trevino, J. Contreras, S. Yang, L. Song, T. Yoshioka, H.-K. Lee, and A. Kirkwood, "Associative hebbian synaptic plasticity in primate visual cortex," *Journal of Neuroscience*, vol. 34, no. 22, pp. 7575–7579, 2014.
- [18] P. U. Diehl, G. Zarella, A. Cassidy, B. U. Pedroni, and E. Neftci, "Conversion of artificial recurrent neural networks to spiking neural networks for low-power neuromorphic hardware," in *2016 IEEE International Conference on Rebooting Computing (ICRC)*. IEEE, 2016, pp. 1–8.
- [19] A. Jacot, F. Gabriel, and C. Hongler, "Neural tangent kernel: Convergence and generalization in neural networks," in *Advances in neural information processing systems*, 2018, pp. 8571–8580.
- [20] K. Huang, Y. Wang, M. Tao, and T. Zhao, "Why do deep residual networks generalize better than deep feedforward networks?—a neural tangent kernel perspective," *arXiv preprint arXiv:2002.06262*, 2020.
- [21] Z. Chen, Y. Cao, Q. Gu, and T. Zhang, "A generalized neural tangent kernel analysis for two-layer neural networks," *Advances in Neural Information Processing Systems*, vol. 33, 2020.
- [22] U. Şimşekli, O. Sener, G. Deligiannidis, and M. A. Erdogdu, "Hausdorff dimension, stochastic differential equations, and generalization in neural networks," *arXiv preprint arXiv:2006.09313*, 2020.
- [23] M. Gurbuzbalaban, U. Şimşekli, and L. Zhu, "The heavy-tail phenomenon in sgd," *arXiv preprint arXiv:2006.04740*, 2020.
- [24] R. Wang, D. Mahajan, and V. Ramanathan, "What leads to generalization of object proposals?" *arXiv preprint arXiv:2008.05700*, 2020.
- [25] M. D. Zeiler and R. Fergus, "Visualizing and understanding convolutional networks," in *European conference on computer vision*. Springer, 2014, pp. 818–833.
- [26] J. Donahue, Y. Jia, O. Vinyals, J. Hoffman, N. Zhang, E. Tzeng, and T. Darrell, "Decaf: A deep convolutional activation feature for generic visual recognition," in *International conference on machine learning*, 2014, pp. 647–655.
- [27] J. Yosinski, J. Clune, Y. Bengio, and H. Lipson, "How transferable are features in deep neural networks?" in *Advances in neural information processing systems*, 2014, pp. 3320–3328.

- [28] T. K. Leen, R. Friel, and D. Nielsen, "Approximating distributions in stochastic learning," *Neural networks*, vol. 32, pp. 219–228, 2012.
- [29] U. Simsekli, O. Sener, G. Deligiannidis, and M. A. Erdogdu, "Hausdorff dimension, heavy tails, and generalization in neural networks," *Advances in Neural Information Processing Systems*, vol. 33, 2020.
- [30] D. Kappel, S. Habenschuss, R. Legenstein, and W. Maass, "Synaptic sampling: A bayesian approach to neural network plasticity and rewiring," in *Advances in Neural Information Processing Systems*, 2015, pp. 370–378.
- [31] U. Simsekli, L. Sagun, and M. Gurbuzbalaban, "A tail-index analysis of stochastic gradient noise in deep neural networks," *arXiv preprint arXiv:1901.06053*, 2019.
- [32] B. M. Hill, "A simple general approach to inference about the tail of a distribution," *The annals of statistics*, pp. 1163–1174, 1975.
- [33] J. Pickands III *et al.*, "Statistical inference using extreme order statistics," *the Annals of Statistics*, vol. 3, no. 1, pp. 119–131, 1975.
- [34] S. Mittnik and S. T. Rachev, "Tail estimation of the stable index α ," *Applied Mathematics Letters*, vol. 9, no. 3, pp. 53–56, 1996.
- [35] V. Paulauskas and M. Vaičiulis, "Once more on comparison of tail index estimators," *arXiv preprint arXiv:1104.1242*, 2011.
- [36] M. Mohammadi, A. Mohammadpour, and H. Ogata, "On estimating the tail index and the spectral measure of multivariate α -stable distributions," *Metrika*, vol. 78, no. 5, pp. 549–561, 2015.
- [37] Y. Gal and Z. Ghahramani, "Dropout as a bayesian approximation: Representing model uncertainty in deep learning," in *international conference on machine learning*, 2016, pp. 1050–1059.
- [38] C. Lee, S. S. Sarwar, P. Panda, G. Srinivasan, and K. Roy, "Enabling spike-based backpropagation for training deep neural network architectures," *Frontiers in Neuroscience*, vol. 14, 2020.
- [39] D. Miller, L. Nicholson, F. Dayoub, and N. Sünderhauf, "Dropout sampling for robust object detection in open-set conditions," in *2018 IEEE International Conference on Robotics and Automation (ICRA)*. IEEE, 2018, pp. 1–7.
- [40] T.-Y. Lin, M. Maire, S. Belongie, J. Hays, P. Perona, D. Ramanan, P. Dollár, and C. L. Zitnick, "Microsoft coco: Common objects in context," in *European conference on computer vision*. Springer, 2014, pp. 740–755.
- [41] D. Miller, F. Dayoub, M. Milford, and N. Sünderhauf, "Evaluating merging strategies for sampling-based uncertainty techniques in object detection," in *2019 International Conference on Robotics and Automation (ICRA)*. IEEE, 2019, pp. 2348–2354.
- [42] M. Horowitz, "1.1 computing's energy problem (and what we can do about it)," in 2014 IEEE International Solid-State Circuits Conference Digest of Technical Papers (ISSCC), in *IEEE, feb*, 2014.
- [43] J. Hosang, R. Benenson, P. Dollár, and B. Schiele, "What makes for effective detection proposals?" *IEEE transactions on pattern analysis and machine intelligence*, vol. 38, no. 4, pp. 814–830, 2015.